Plant Physiology and Biochemistry 135 (2019) 149–159

Contents lists available at ScienceDirect

Plant Physiology and Biochemistry

journal homepage: www.elsevier.com/locate/plaphy

Research article

Investigating the physiological mechanisms underlying *Salicornia ramosissima* response to atmospheric CO_2 enrichment under coexistence of prolonged soil flooding and saline excess

Jesús Alberto Pérez-Romero[a,*], Bernardo Duarte[b], Jose-Maria Barcia-Piedras[c], Ana Rita Matos[d], Susana Redondo-Gómez[a], Isabel Caçador[c], Enrique Mateos-Naranjo[a]

[a] Departamento de Biología Vegetal y Ecología, Facultad de Biología, Universidad de Sevilla, 1095, 41080, Sevilla, Spain
[b] MARE - Marine and Environmental Sciences Centre, Faculty of Sciences of the University of Lisbon, Campo Grande, 1749-016, Lisbon, Portugal
[c] Department of Ecological Production and Natural Resources Center IFAPA Las Torres-Tomejil Road Sevilla - Cazalla Km 12'2, 41200, Alcalá del Río, Seville, Spain
[d] BioISI—Biosystems and Integrative Sciences Institute, Plant Functional Genomics Group, Departamento de Biologia Vegetal, Faculdade de Ciências da Universidade de Lisboa, Campo Grande, 1749-016, Lisboa, Portugal

ARTICLE INFO

Keywords:
Climate change
Fluorescence
Gas exchange
Halophyte
Salinity
Water logging

ABSTRACT

A 45-days long climatic chamber experiment was design to evaluate the effect of 400 and 700 ppm atmospheric CO_2 treatments with and without soil water logging in combination with 171 and 510 mM NaCl in the halophyte *Salicornia ramosissima*. In order to ascertain the possible synergetic impact of these factors associate to climatic change in this plant species physiological and growth responses. Our results indicated that elevated atmospheric CO_2 concentration improved plant physiological performance under suboptimal root-flooding and saline conditions plants. Thus, this positive impact was mainly ascribed to an enhancement of energy transport efficiency, as indicated the greater P_G, N and Sm values, and the maintaining of carbon assimilation capacity due to the higher net photosynthetic rate (A_N) and water use efficiency ($_i$WUE). This could contribute to reduce the risk of oxidative stress owing to the accumulation of reactive oxygen species (ROS). Moreover, plants grown at 700 ppm had a greater capacity to cope with flooding and salinity synergistic impact by a greater efficiency in the modulation in enzyme antioxidant machinery and by the accumulation of osmoprotective compounds and saturated fatty acids in its tissues. These responses indicate that atmospheric CO_2 enrichment would contribute to preserve the development of *Salicornia ramosissima* against the ongoing process of increment of soil stressful conditions linked with climatic change.

1. Introduction

The most recent climate change predictions indicate that it will impose significant increases in the global average air and sea surface temperatures by about 2.5 °C (IPCC, 2001) together with an increase of atmospheric CO_2 concentration to value of c. 760 ppm by 2100. Due to this global warming, sea level rise (SLR) and soil salinization will be some of the major side-effects, as a result of polar ice meltdown and the increment of surface water evaporation, respectively (IPCC, 2001). There is a consensus on the direct physiological impact of increasing CO_2 concentration on plant photosynthesis and metabolism, stimulating growth and development in hundreds of plants species (Ghannoum et al., 2000). However, the information is very scarce in relation with the effect of atmospheric CO_2 enrichment on photosynthesis in plants subjected to a complex environmental matrix. Therefore, the majority of studies that have tried to address this concern were designed to explore as much two environmental factor interactions; i.e. the effect of rising CO_2 along with salinity (Lenssen et al., 1993; Rozema, 1993; Geissler et al., 2009a, 2015, 2009b; Mateos-Naranjo et al., 2010a, 2010b; Pérez-Romero et al., 2018), drought (Yang et al., 2014; Slama et al., 2015; Calvo et al., 2017), temperature (Bernacchi et al., 2006) or flooding (Duarte et al., 2014), etc. Only few studies have addressed the impact of more than two coexisting factors (Lenssen et al., 1995). Although the majority of them only performed shallow physiological evaluations being difficult to find a complete analysis of photosynthetic responses taking into account carbon assimilation capacity and energy use efficiency together with other metabolism processes, such as antioxidant enzyme modulation, involved in the plants responses to environmental stress.

Salicornia ramosissima J. Woods (Chenopodiaceae), represent a

* Corresponding author. Dpto. Biología Vegetal y Ecología, Facultad de Biología, Universidad de Sevilla, Av Reina Mercedes s/n, 41012, Sevilla, Spain.
E-mail address: jperez77@us.es (J.A. Pérez-Romero).

https://doi.org/10.1016/j.plaphy.2018.12.003
Received 14 August 2018; Received in revised form 13 November 2018; Accepted 3 December 2018
Available online 06 December 2018
0981-9428/

Abbreviations

WL	Water logging
RGR	Relative growth rate
WC	Water content
Ψ_o	Osmotic potential
A_N	Net photosynthetic rate
g_s	Stomatal conductance
C_i	Intercellular CO_2 concentration
iWUE	Intrinsic water use efficiency
ETR_{max}	Maximum electron transport rate
PSII	Photosystem II
F_v/F_m	Maximum quantum efficiency of PSII photochemistry
Φ_{PSII}	PS II Operational and Maximum Quantum Yield
GPX	Guaiacol peroxidase enzymatic activity
SOD	Superoxide dismutase enzymatic activity
ROS	Reactive oxygen species
SFA	Saturated fatty acids
UFA	Unsaturated fatty acids
MUFA	Monounsaturated fatty acids
PUFA	Poliunsaturated fatty acids
DBI	Double bond index

suitable model plant to study in detail the effect of atmospheric CO_2 enrichment on the physiological responses of a plant species under co-existing suboptimal environmental conditions, such as soil flooding and salinity conditions. Since this species is a C_3 halophyte which inhabits salt marshes and inland salty habitats like shores of salt lakes being able to tolerate a wide range of salinity and a certain degree of immersion (Davy et al., 2001). However, these estuarine areas will be particularly vulnerable to SLR (Reed, 2002; Duarte et al., 2014) and salinization events (IPCC, 2007). Our recent study showed that CO_2 enrichment improves *S. ramosissima* response to suboptimal salinity conditions through an overall protection of its photosynthetic pathway (Pérez-Romero et al., 2018), but non-attention have been paid in SLR risk.

Therefore, this study was designed and conducted to fill this gap of knowledge. In particular, we asked the following questions: (i) Would atmospheric CO_2 enrichment have a positive impact on *S. ramosissima* physiological performance under co-occurrence of different stress factors, such as prolonged soil flooding and salinity? (ii) Would this effect be different to previous described only in presence of salinity, especially at the level of specific steps of photosynthetic pathway? (iii) Would other metabolism processes, such as antioxidant enzyme machinery or fatty acids profiles modulation, be involved in these differential responses?

2. Material and methods

2.1. Plant material

Seeds of *S. ramosissima* were collected in September 2016 from a well stablished population located in Odiel marshes (37°15'N, 6°58'O; SW Spain). Then, collected seed were placed into a germinator (ASL Aparatos Científicos M-92004, Madrid, Spain) and subjected to a day-night regime of 16 h of light (photon flux rate, 400–700 nm, 35 μmol m^{-2} s^{-1}) at 25 °C and 8 h of darkness at 12 °C, for 15 days. After germination, seedlings were planted in individual plastic plots (9 cm high x 11 cm diameter) filled with pearlite as substrate, and moved to a greenhouse with controlled conditions (temperature between 21 and 25 °C, 40–60% relative humidity and natural daylight 250–1000 μmol m^{-2} s^{-1} light flux). The pots were placed in shallow trays watering with 20% Hoagland's solution (Hoagland and Arnon, 1938) and 171 mM NaCl (Pérez-Romero et al., 2016). Plants were kept under the previously described conditions until the beginning of the experiment.

2.2. Experimental treatments

After 3 months of seedlings culture, when plants had a mean height c. 13 cm, pearlite was washed off and plants were transferred to individual plastic pots of 0.25 l containing an organic commercial substrate (Gramoflor GmbH und Co. KG.) and sand mixture (2:1) in order to facilitate water level treatment. Pots were randomly divided in eight experimental blocks with eleven plants in each one, as follow: two atmospheric CO_2 concentrations (400 ppm and 700 ppm) in combination with two water levels (water logging, WL and no water logging, noWL) and two salinity concentrations (171 and 510 mM NaCl). These conditions were kept for 45 days in order to obtain a more realistic approximation about the maximum permanent inundation period that we have observed during field surveys in natural populations of *S. ramosissima* which inhabits inland salty habitats (data not published). In addition, being an annual specie, this period was used to avoid a decreased in the physiology variables due to age because after the 3 months of seedlings culture the plants where around 135 days old.

Salinity treatments, 171 and 510 mM NaCl, were established by using tap water and NaCl of the appropriate concentration. In addition, these solutions were added to each tray to get water treatments. Thus, for the WL treatment, water level was continuous maintained at soil surface level, and for no WL treatment water level was continuous covering 2 cm from the bottom of the tray. Finally, for the atmospheric CO_2 concentration treatments pots were placed in controlled-environment chambers (Aralab/Fitoclima 18.000 EH, Lisbon, Portugal) with alternating diurnal regime of 14 h of light and 25 °C and 10 h of darkness and 18 °C and relative humidity between 40 and 60% and atmospheric CO_2 control. Atmospheric CO_2 concentrations in chambers were continuously recorded by CO_2 sensors (Aralab, Lisbon, Portugal) and maintained by supplying pure CO_2 from a compressed gas cylinder (Air liquide, B50 35 K). As well as the salinity and water levels to avoid changes due to evaporation.

2.3. Growth analysis

At the beginning of the experiment just before treatments imposition belowground and aboveground fractions of 10 randomly selected plants were separated, dried at 80 °C for 48 h and weighed. At the end of the essay, 8 plants per treatment were processed in the same way. The relative growth rate (RGR) was calculated using the formula:

$$RGR = (\ln Bf - \ln B_i)\, D^{-1}\ (g\ g^{-1}\ day^{-1})$$

Where Bf = final dry mass (an average eight plants per treatment), B_i = initial dry mass (an average of the ten plants dried at the beginning of the experiment) and D = duration of experiment (days).

2.4. Plant water status

Water content (WC) of primary branches (n = 8, per treatment) were calculated after 45 days of treatment as follow:

$$WC = ((FW - DW) / FW)\ 100$$

Where FW = fresh weight of the branches and DW = dry weight after oven-drying at 80 °C for 48 h.

On the other hand, the osmotic potential (Ψ_o) of primary branches (n = 5, per treatment) was determined 45 days after the onset of the treatments, using psychrometric technique with a Vapour Pressure Osmometer (5600 Vapro, Wescor, Logan, USA).

2.5. Measurement of gas exchange

Instantaneous gas exchange measurements were taken on randomly selected primary branches of individual plants (n = 7, per treatment) using an infrared gas analyser in an open system (LI-6400, LI-COR Inc., Neb., USA) equipped with a light leaf chamber (Li-6400-02B, Li-Cor Inc.) after 45 days of treatment. Net photosynthetic rate (A_N), stomatal conductance (g_s), intercellular CO_2 concentration (C_i) and intrinsic water use efficiency ($_i$WUE) were determined under the follow leaf cuvette conditions: a photosynthetic photon flux density (PPFD) 1000 μmol photon m^{-2} s^{-1} (with 15% blue light to maximize stomatal aperture), vapour pressure deficit of 2.0–3.0 kPa, air temperature of 25 ± 2 °C, relative humidity of 50 ± 2% and CO_2 concentration surrounding leaf (C_a) of 400 and 700 μmol mol^{-1} air for plants exposed to 400 and 700 ppm CO_2, respectively. Photosynthetic area was calculated as half the area of the cylindrical branches, as only the upper half received the unilateral illumination in the leaf chamber (Redondo-Gómez et al., 2010). Intrinsic water use efficiency ($_i$WUE) was calculated as the ratio between A_N and g_s.

2.6. Chlorophyll fluorescence

Modulated chlorophyll fluorescence measurements were performed at the same time as gas exchange measures on the same branches of gas exchange using a FluorPen FP100 (Photo System Instruments, Czech Republic) on light and 30 min dark-adapted primary branches after 45 days of treatment (n = 7, per treatment). Light energy yields of photosystem II (PS II) reaction centres were determined with a saturation pulse method as Schreiber et al. (1986) described. The maximum fluorescence signal across time was estimated by using a saturating light pulse of 0.8 s with an intensity of 8000 μmol m^{-2} s^{-1}. The minimum fluorescence (F'_0), the maximum fluorescence (F'_m) and the operational photochemical efficiency values of light and dark adapted branches were compared. Quantum yield of PS II (QY) and relative Quantum yield of PS II (Q'Y) were calculated as F_v/F_m and Φ_{PSII} respectively. Maximum electron transport rate (ETR_{max}) and the Kausky curves, or JIP-test, which depicts the rate of reduction kinetics of various components of PSII, were also measured in dark-adapted branches (n = 5, per treatment) according to Duarte et al. (2015). For this purpose, the pre-programmed RLC and OJIP protocols of the FluorPen were used. All derived parameters for both RLC and OJIP were calculated according to Marshall et al. (2000) and Strasser et al. (2004) respectively (Table 1). Finally, ETR_{max}/A_N ratio was calculated with the values obtained from fluorescence rapid light curves, RLC (see below) and instantaneous gas exchange measurements.

2.7. Anti-oxidant enzymatic activity

Enzyme extraction was done following the method used by Duarte et al. (2015). At the end of experiment, 500 mg of fresh branches samples were grounded in 8 ml of 50 mM sodium phosphate buffer (pH 7.6) with 0.1 mM Na-EDTA and were centrifuged at 10.000 rpm for 20 min at 4 °C to obtained the soluble proteins. Three samples per treatment were used and three measurements per sample were registered. Protein content in the extracts was obtained according to Bradford (1976), using bovine serum albumin as a standard.

Guaiacol peroxidase EC 1.11.1.7 (GPX) was calculated as Bergmeyer (1974) indicated. With a reaction mixture made of 50 mM of sodium phosphate buffer (pH 7.0), 2 mM of H_2O_2 and 20 mM of guaiacol. For all this enzymatic activities 100 μL of vegetal extract was added at the reaction mixture to start the reaction. Superoxide dismutase EC 1.15.1.1 (SOD) activity was assayed by monitoring the reduction of pyrogallol at 325 nm following Marklund and Marklund (1974) work. The reaction mixture was 50 mM of sodium phosphate buffer (pH 7.6), 0.1 mM of Na-EDTA, 3 mM of pyrogallol, Mili-Q water. The reaction was started with the addition of 10 μL of enzyme extract. Auto-oxidation of the substrates was evaluated by control samples with the reaction mixture but without the enzyme extract.

2.8. Betain concentration

Betain were determined as the main osmocompatible solute present in succulent halophytes (Duarte et al., 2013). To quantify the betain concentration 500 mg samples of fresh branches were collected at the end of the essay and freeze-dried for 48 h. Then, the samples were grinded and left in ultra-pure water for 24 h. After that, the sample extract was diluted 1:1 with 2 N H_2SO_4. Cold KI-I_2 reagent (0.20 ml) was mixed with 0.5 ml of the diluted sample. The tubes were stored at 4 °C for 16 h and then centrifuged at 10.000 rpm for 15 min at 0 °C. The supernatant was carefully aspirated with a fine tipped glass tube. The

Table 1
Summary of fluorometric analysis parameters and their description.

Photosystem II Efficiency	
Fv/Fm	Maximum quantum efficiency of PSII photochemistry
PS II Operational and Maximum Quantum Yield (ΦPSII)	Light and dark-adapted quantum yield of primary photochemistry, equal to the efficiency by which a PS II trapped photon will reduce Q_A to Q_A^-
Rapid Light Curves (RLCs)	
ETR_{max}	Maximum ETR after which photo-inhibition can be observed
Energy Fluxes (Kautsky curves)	
Area	Corresponds to the oxidized quinone pool size available for reduction and is a function of the area above the Kautsky plot
φ_{P0}	Maximum yield of primary photochemistry
φ_{E0}	Probability that an absorbed photon will move an electron into the electronic transport chain
φ_{D0}	Quantum yield of the non-photochemical reactions
Ψ_0	Probability of a PS II trapped electron to be transported from Q_A to Q_B
δR_0	Electron movement efficiency from the reduced intersystem electron acceptors to the PSI and electron acceptors.
N	Reaction centre turnover rate
Sm	Relative pool size of PQ.
M_0	Net rate of PS II RC closure.
ABS/CS	Absorbed energy flux per leaf cross-section.
TR/CS	Trapped energy flux per leaf cross-section
ET/CS	Electron transport energy flux per leaf cross-section
DI/CS	Dissipated energy flux per leaf cross-section.
RC/CS	Number of available reaction centres per leaf cross section
Grouping Probability (P_G)	The grouping probability is a direct measure of the connectivity between the two PS II units (Strasser and Stribet, 2001)

periodide crystals produced were dissolved in 9.0 ml of 1,2-dichloroethane (reagent grade). After 2–2.5 h, the absorbance was measured at 365 nm with a Hitachi Spectrometer model 100–20 (Grieve and Grattan, 1983).

2.9. Fatty acid profile

At the end of the experiment, 150 mg samples of fresh and green branches were taken to determine the fatty acids composition. The method used was the direct acidic trans-esterification previously described by Matos et al. (2007). A gas chromatograph (3900 Gas Chromatograph; Varian, Palo Alto, CA, USA) equipped with a hydrogen flame-ionisation detector was used to separate the fatty acid methyl esters (FAME) with a fused silica 0.25 mm i.d. x 50 m capillary column (WCOT Fused Silica, CP-Sil 88 for FAME; Varian). The internal standard was heptadecanoate (C17:0). Double-bond index (DBI) was calculated as:

DBI = ((16:1t% + 18:1%) + (2*18:2%) + (3*18:3%)) * 100

Where 16:1t% was the percentage of palmitoleic fatty acid, 18:1% the percentage of oleic fatty acid, 18:2% the percentage of linoleic fatty acid and 18:3% the percentage of omega-3 fatty acid.

2.10. Statistical analysis

Statistical software package R was used to perform the entire statistic. A multivariate statistical approach using a principal component analysis model was performed to get an overview of the plant development, physiological and biochemical status in response to the different experimental treatments. Then, a downscaling assess was carried out through to generalized linear models (GLM) to analyze the interactive effects of atmospheric CO_2 concentration, water level and NaCl concentrations (as categorical factors) on the growth, physiological and biochemical parameters (as dependent variables) of *S. ramosissima* plants. Multiple comparisons were analysed by a LSD (post hoc) test. Before statistical analysis, Kolmogorov-Smirnov and Levene tests were used to verify the assumptions of normality and homogeneity of variances, respectively.

3. Results

3.1. Multivariate approach: global overview of physiological and biochemical status

PCA ordination provided an overall picture of the physiological/biochemical condition of *S. ramosissima* during the experimental setup explaining 64% of the proportion of variation of the recorded data (i.e. Axis 1 and Axis 2 a 43% and a 21%, respectively; Fig. 1). Hence, the bidimensional plot revealed a certain divergence between both atmospheric CO_2 concentration treatments along axis 2, with most of non-CO_2 enrichment plants located in the upper part (Fig. 1A). This separation by CO_2 treatment was mainly explained by higher A_N, C_i, $_i$WUE, Ψ_o, SOD activity and SFA accumulation at 700 ppm CO_2 compared to 400 ppm CO_2 (Fig. 1B). In addition, PCA analysis reflected a clear divergence of plants grown at 700 ppm CO_2 + WL + 510 mM NaCl in the left part of the plot linked with the greater P_G, N, Sm, φ_{D0}, DI/CS and Betain concentration compared with the rest of treatments (Fig. 1A and B).

Table 2
Relative growth rate (RGR), water content (WC) and absolute value of osmotic potential (Ψ_o) (MPa) state in randomly selected branches of *Salicornia ramosissima* in response to treatment with two atmospheric CO_2 concentrations (400 ppm and 700 ppm) in combination with two water levels (water logging, WL and no water logging, noWL) and two salinity concentrations (171 and 510 mM NaCl) for 45 days. Values represent mean ± SE, n = 8 for RGR and WC and n = 5 for Ψ_o. (GLM, [CO_2] x WLx [NaCl]; LSD test, $P < 0.05$). [CO_2],WL, NaCl or [CO_2]xWLxNaCl indicate main or interaction significant effects ($^{*}P < 0.01$, $^{**}P < 0.001$, $^{***}P < 0.0001$).

[CO_2]	Water level	[NaCl]	RGR^{WL*}	WC	$\Psi_o^{[CO2]*[NaCl]**}$
400	no WL	171	0.104 ± 0.01	87.1 ± 1.0	3.38 ± 0.06
		510	0.093 ± 0.01	85.8 ± 0.3	4.94 ± 0.09
	WL	171	0.095 ± 0.01	86.9 ± 0.8	4.14 ± 0.08
		510	0.096 ± 0.01	87.8 ± 0.3	4.24 ± 0.06
700	no WL	171	0.113 ± 0.01	86.0 ± 0.4	3.05 ± 0.18
		510	0.118 ± 0.00	84.9 ± 0.9	4.71 ± 0.11
	WL	171	0.098 ± 0.01	87.0 ± 0.8	2.99 ± 0.07
		510	0.100 ± 0.01	86.3 ± 0.3	4.14 ± 0.07

3.2. Growth analysis

RGR values were greater overall in plants exposed to 700 ppm CO_2 than their non-CO_2 enrichment counterpart, obtaining the highest values in plants grown at 700 ppm CO_2 + noWL at both NaCl concentrations; however this positive effect was in certain degree mitigated under WL conditions (GLM: $_{WL,}$ $p < 0.05$; Table 2).

3.3. Plant water status

Water content (WC) did not vary with atmospheric CO_2 concentration, water logging and salinity, showing in all cases values c. 86% (Table 2). Contrarily, there were significant effects of atmospheric CO_2 concentration and salinity on the osmotic potential (Ψ_o) but no

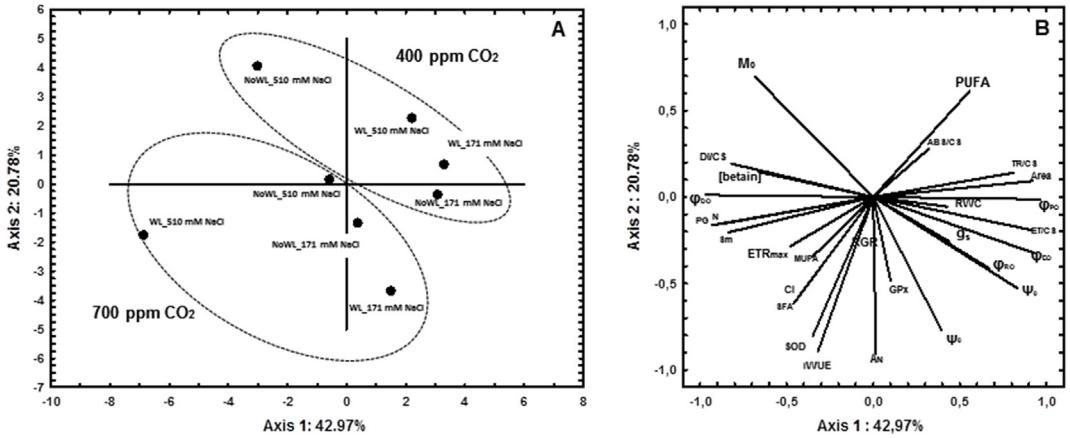

Fig. 1. PCA biplot of the physiological and biochemical data of *Salicornia ramosissima* plants in the experimental set-up. Loading plots for the first axis (explained variation is 42.97%) and second axis (explained variation is 20.78%).

significant interactions (GLM: $_{[CO2],}$ $p < 0.001$; $_{[NaCl]}$, $p < 0.05$; Table 2). Thus, Ψ_o increased at 510 mM NaCl being this increment overall reduced at elevated CO_2 concentration, independently of WL level (Table 2).

3.4. Gas exchange measurements

There were significant effects of atmospheric CO_2 concentration, WL and salinity on net photosynthetic rate (A_N) after 45 d of treatment, but no synergistic effect could be identified (GLM: $_{[CO2],\ WL,\ [NaCl]}$, $p < 0.05$). Thus, plants grown at higher CO_2 concentration showed slightly higher values of A_N than their 400-ppm CO_2 counterparts; being this augmentation more evident under water logging conditions compared with the remaining treatments. In addition, there was a decrease in A_N at 510 mM NaCl, but less pronounced at high CO_2 concentration and in presence of water logging (Fig. 2A). Furthermore, stomatal conductance (g_s) values were lower at elevated atmospheric CO_2 concentration and at 510 mM NaCl in noWL plants (GLM: $_{[CO2],\ WL,\ [NaCl]}$, $p < 0.05$; Fig. 2B). Overall, intercellular CO_2 concentration (C_i) values were greater in plants grown at 700 ppm CO_2 independently of saline and water logging conditions (GLM: $_{[CO2],}$ $p < 0.01$; Fig. 2C). Finally, $_i$WUE was only affected by CO_2 concentration with higher values for plants grown at 700 ppm CO_2 (GLM: $_{[CO2],}$ $p < 0.01$; Fig. 2D).

3.5. Fluorescence measurements

F_v/F_m and Φ_{PSII} values did not show any significant differences between atmospheric CO_2 concentration, WL or salinity treatments showing mean values of between 0.68–0.63 and between 0.64 and 0.65 for F_v/F_m and Φ_{PSII}, respectively (data not shown). However, there was a significant effect of atmospheric CO_2 concentration on ETR_{max} with higher values at 700 ppm CO_2 (GLM: $_{[CO2],}$ $p < 0.001$; Fig. 2E). Also, there was a synergistic effect of the three factors studied on ETR_{max}/A_N, thus this ratio increased in plants grown at 510 mM NaCl but this increment was mitigated at elevated atmospheric CO_2 concentration and plants exposed to WL conditions (GLM: $_{[CO2]\ x\ WL\ x\ [NaCl]}$, $p < 0.01$; Fig. 2F).

Focusing on the derived-parameters from the Kautsky curves, there was not a clear pattern of response to atmospheric CO_2 concentration, WL and salinity treatments. This lack of pattern was seeing at the oxidized quinone pool size available for reduction (Area), net rate of PS II RC closure (M_0), electron movement efficiency from the reduced intersystem electron acceptors to the PSI and electron acceptors (δR_0), maximum yield of primary photochemistry (φ_{P0}), probability of a PS II trapped electron to be transported from Q_A to Q_B (Ψ_0), probability that an absorbed photon will move an electron into the electronic transport chain (φ_{E0}), quantum yield of the non-photochemical reactions (φ_{D0}) (Fig. 3A, B, E, F and Fig. 4A–D). Nevertheless, grouping probability (P_G), reaction centre turnover rate (N) and relative pool size of PQ (Sm) values increased markedly in plants grown at 700 ppm CO_2 and elevated water and salinity levels compared with the rest of treatments (GLM: $_{[CO2]\ x\ WL\ x\ [NaCl]}$, $p < 0.05$; Fig. 3B, C, D). Finally, regarding the energetic fluxes on a leaf cross-section basis (phenomological fluxes) showed that absorbed (ABS/CS), trapped (TR/CS), dissipated (DI/CS)

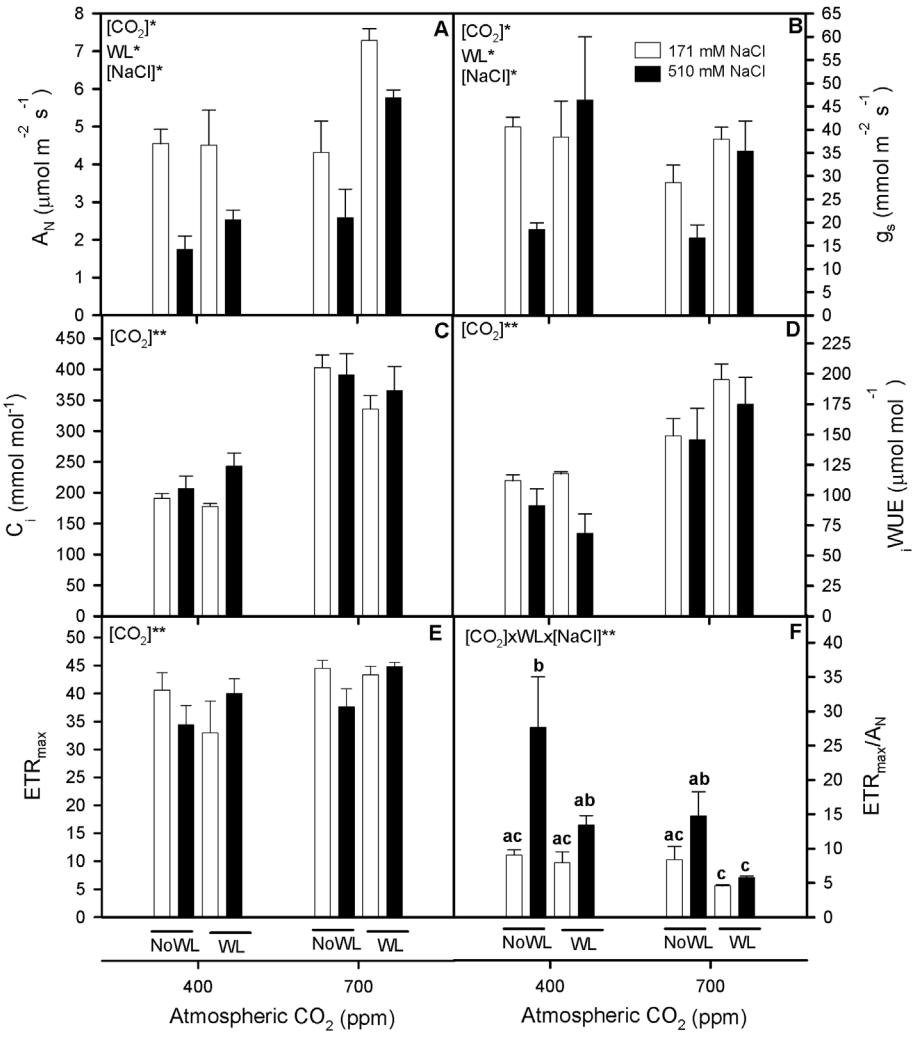

Fig. 2. Net photosynthetic rate, A_N (A), stomatal conductance, g_s (B), intercellular CO_2 concentration, C_i (C), intrinsic water use efficiency ($_i$WUE) (D), maximum ETR after which photo-inhibition can be observed (ETR_{max}) (E) and ETR_{max} net photosynthetic rate ratio, ETR_{max}/A_N (F) in randomly selected, primary branches of *Salicornia ramosissima* in response to treatment with two atmospheric CO_2 concentrations (400 ppm and 700 ppm) in combination with two water levels (water logging, WL and no water logging, noWL) and two salinity concentrations (171 and 510 mM NaCl) for 45 days. Values represent mean ± SE, n = 7. Different letters indicate means that are significantly different from each other (GLM, $[CO_2]$ x WLx [NaCl]; LSD test, $P < 0.05$). $[CO_2]$,WL, [NaCl] or $[CO_2]$ x WL x [NaCl] in the corner of the panels indicate main or interaction significant effects ($^*P < 0.01$, $^{**}P < 0.001$, $^{***}P < 0.0001$).

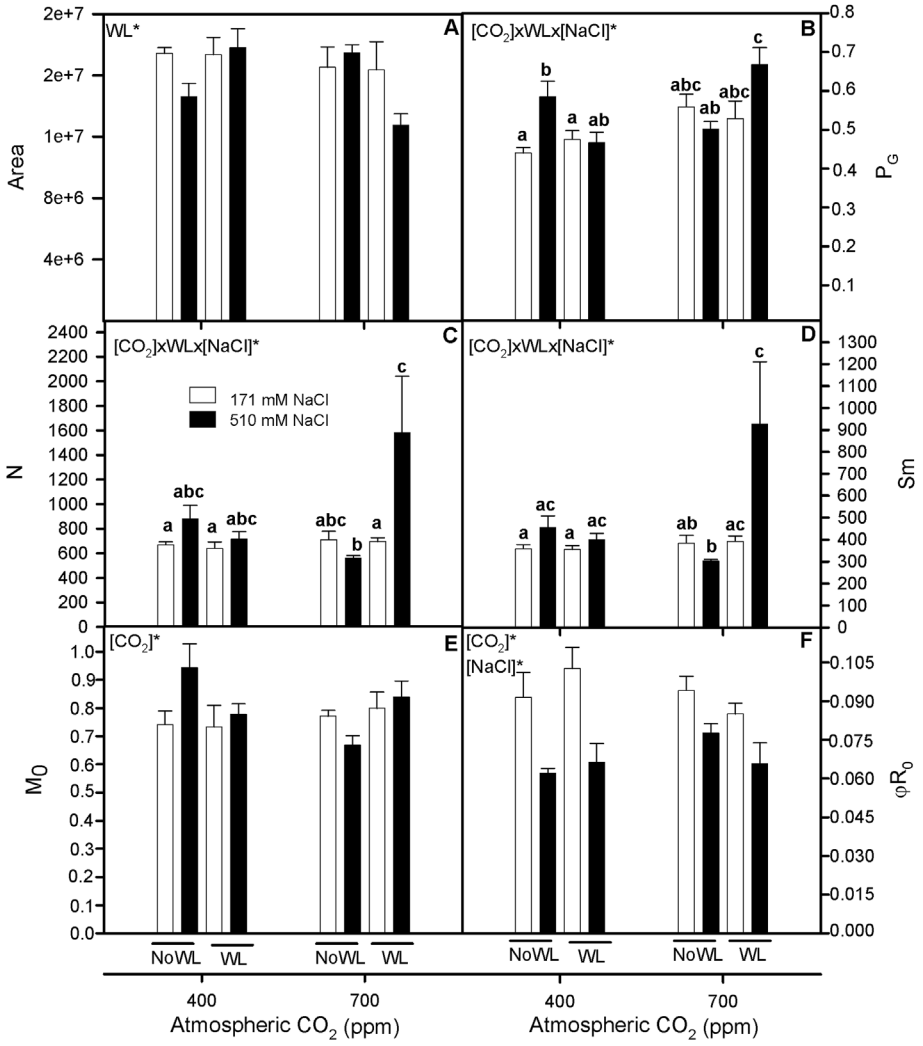

Fig. 3. Area (A), grouping probability (P_G) (B), reaction centre turnover rate (N) (C), relative PQ pool size (Sm) (D), net rate of PS II RC closure (M_0) (E) and maximum yield of primary photochemistry, (φ_{R0}) (F) in dark adapted randomly selected, primary branches of *Salicornia ramosissima* in response to treatment with two of NaCl concentrations (171 and 510 mM) and with water logging (WL) and with no water logging (noWL) at 400 and 700 ppm CO_2 after 45d of treatment. Values represent mean ± SE, n = 7. Different letters indicate means that are significantly different from each other (GLM, $[CO_2]$ x WLx [NaCl]; LSD test, $P < 0.05$). $[CO_2]$,WL, [NaCl] or $[CO_2]$ x WL x [NaCl] in the corner of the panels indicate main or interaction significant effects ($^{*}P < 0.01$, $^{**}P < 0.001$, $^{***}P < 0.0001$).

and electron transported (ET/CS) for cross section had very similar values in all treatments with no relevant differences between them (Fig. 5A–D).

3.6. Anti-oxidant enzymatic activity and osmocompatible solutes

GP_X enzyme activity did not vary between the plant exposed to the different experimental treatment (Fig. 6A), but SOD presented a clear tendency to be higher when *S. ramosissima* was grown at 700 ppm of CO_2 (GLM $_{[CO2],}$ $p < 0.001$; Fig. 6B): although without WL or salinity treatment variations.

On the other hand, there was a synergistic effect of the three experimental factors in betain concentration (GLM: $_{[CO2]\ x\ WL\ x\ [NaCl]}$, $p < 0.05$). Thus, betain concentration increased considerable at 700 ppm CO_2 in plants grown at 510 mM NaCl at both WL treatments (Fig. 6C).

3.7. Fatty acid composition

Percentage of palmitic acid (C16:0) and linolenic acid (C18:3) were significantly affected by CO_2 (GLM: $_{[CO2],}$ $p < 0.01$). Hence, overall 16:0 percentage was greater at elevated CO_2 concentration for all salinity and WL treatments; while the percentage of C18:3 decreased (Fig. 7A). In both cases, the differences were less evident for low salinity and water level being statistically significant the interactions for palmitic acid (GLM: $_{[CO2]\ x\ WL\ x\ [NaCl]}$, $p < 0.05$). For the remaining fatty acids analysed there were no significant differences between experimental treatments (Fig. 7A). The relative abundance of the saturation classes showed an increase in saturated fatty acid (SFA) and a decrease in the unsaturated classes (UFA, PUFA and MUFA) owing to the increment in atmospheric CO_2 (GLM: $_{[CO2],}$ $p < 0.01$) (Fig. 7B). Unsaturated/saturated ratio (UFA/SFA) (Fig. 7C) showed a significant slightly decrease at high CO_2 atmospheric concentration along with 510 mM NaCl at both WL treatments (GLM: $_{[CO2]\ x\ WL\ x\ [NaCl],}$ $p < 0.05$). Nevertheless, there were no significant effect in PUFA/SFA, 18:2/18:3 and DBI for any of the variables studied (Fig. 7C).

4. Discussion

Understanding the effects of possible interactions between atmospheric CO_2 enrichment and other ecosystems factors on plants species physiological performance is essential for designing more realistic models about the impact of climatic change on plant species development (Bernacchi et al., 2006). This information is particularly important in the most vulnerable ecosystems such as coastal areas and its vegetation, owing to its elevated risk of SLR (Reed, 2002; Duarte et al., 2014) and salinization events (IPCC, 2007).

This study showed that atmospheric CO_2 enrichment could ameliorate the deleterious impact of co-existed water logging and salinity suboptimal growth conditions on the physiological performance of *S. ramosissima*. Thus, plants grown at 700 ppm CO_2, WL and at both salinity levels surpassed the A_N values obtained by the plants grown in

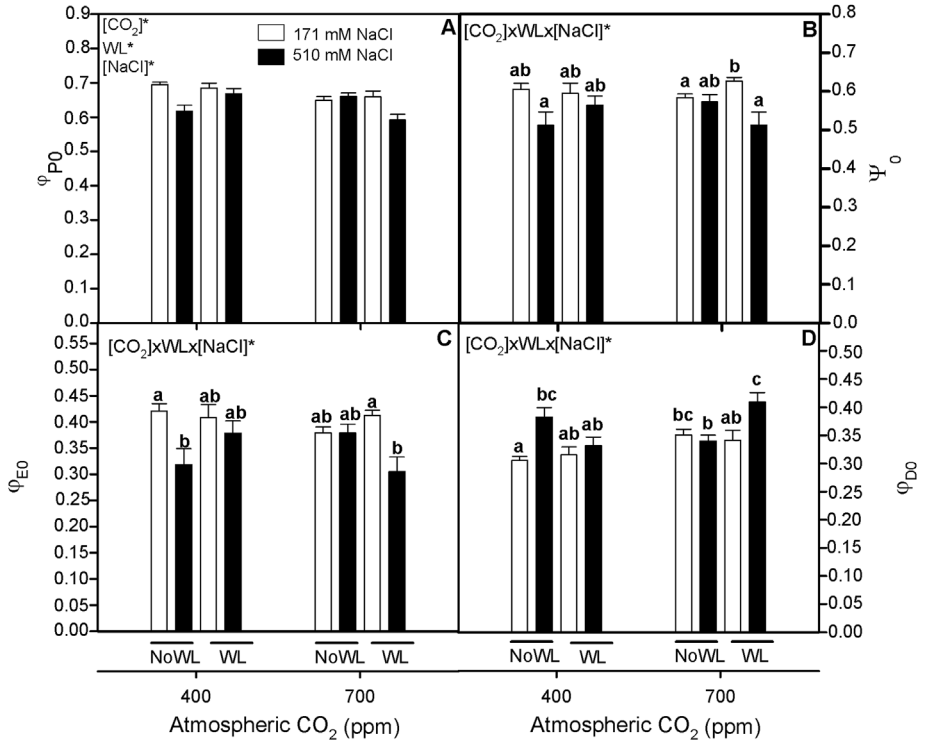

Fig. 4. φ_{P0} (A), Ψ_0 (B), φ_{E0} (C), and φ_{D0} (D) in dark adapted randomly selected, primary branches of *Salicornia ramosissima* in response to treatment with two of NaCl concentrations (171 and 510 mM) and with water logging (WL) and with no water logging (noWL) at 400 and 700 ppm CO_2 after 45d of treatment. Values represent mean ± SE, n = 7. Different letters indicate means that are significantly different from each other (GLM, $[CO_2]$ x WLx [NaCl]; LSD test, $P < 0.05$). $[CO_2]$,WL, [NaCl] or $[CO_2]$ x WL x [NaCl] in the corner of the panels indicate main or interaction significant effects ($^{*}P < 0.01$, $^{**}P < 0.001$, $^{***}P < 0.0001$).

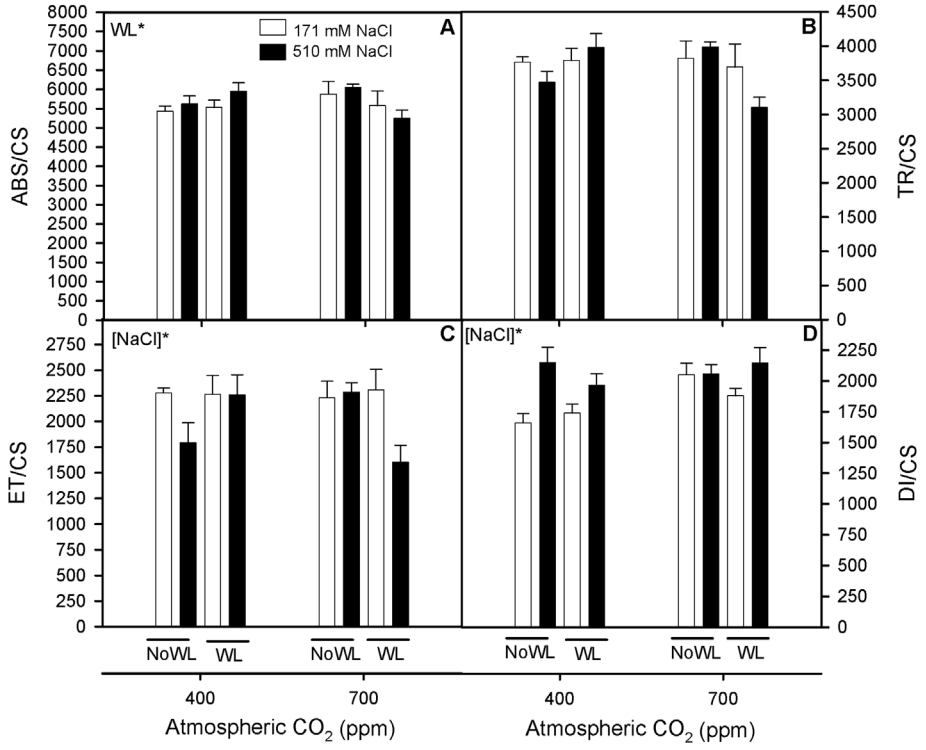

Fig. 5. Absorbed energy fluxtrapped energy flux, ABS/CS (A), trapped TR/CS (B) electron transport energy flux ET/CS (C) and dissipated energy fluxes, DI/CS (D) in dark adapted randomly selected, primary branches of *Salicornia ramosissima* in response to treatment with two of NaCl concentrations (171 and 510 mM) and with water logging (WL) and with no water logging (noWL) at 400 and 700 ppm CO_2 after 45d of treatment. Values represent mean ± SE, n = 7. Different letters indicate means that are significantly different from each other (GLM, $[CO_2]$ x WLx [NaCl]; LSD test, $P < 0.05$). $[CO_2]$,WL, [NaCl] or $[CO_2]$ x WL x [NaCl] in the corner of the panels indicate main or interaction significant effects ($^{*}P < 0.01$, $^{**}P < 0.001$, $^{***}P < 0.0001$).

optimal conditions (i.e no WL and low salinity). Furthermore, g_s values decreased at 510 mM NaCl in no WL plants and overall were lower at elevated CO_2 atmospheric concentration. This reduction could be explained by the increase of C_i originated by the elevated CO_2 concentration; this could promote partial stomatal closure (Robredo et al., 2007). In addition, it is worth to mention that g_s values did not vary respect to values registered in plants grown at noWL + 171 mM NaCl contrary to the drop recorded in A_N at high salinity and WL levels in not CO_2 enrichment plants. This mitigation effect fot g_s of water logging has been previously described by Ullah et al. (2017). Ullah et al. (2017) ascribed it to the water excess which would stimulates the stomatal aperture ameliorating the stomata closure effect of high salinity. This effect was also evident at 700 ppm CO_2 for our treated plants. The general g_s reduction at 700 ppm CO_2 would contribute to preserve the trade-off between CO_2 acquisition for photosynthetic process and water losses in *S. ramosissima* as indicated the higher $_i$WUE values, being this impact especially important at 510 mM NaCl since these plants would be able to cope with the stress derived from salt excess. Robredo et al.

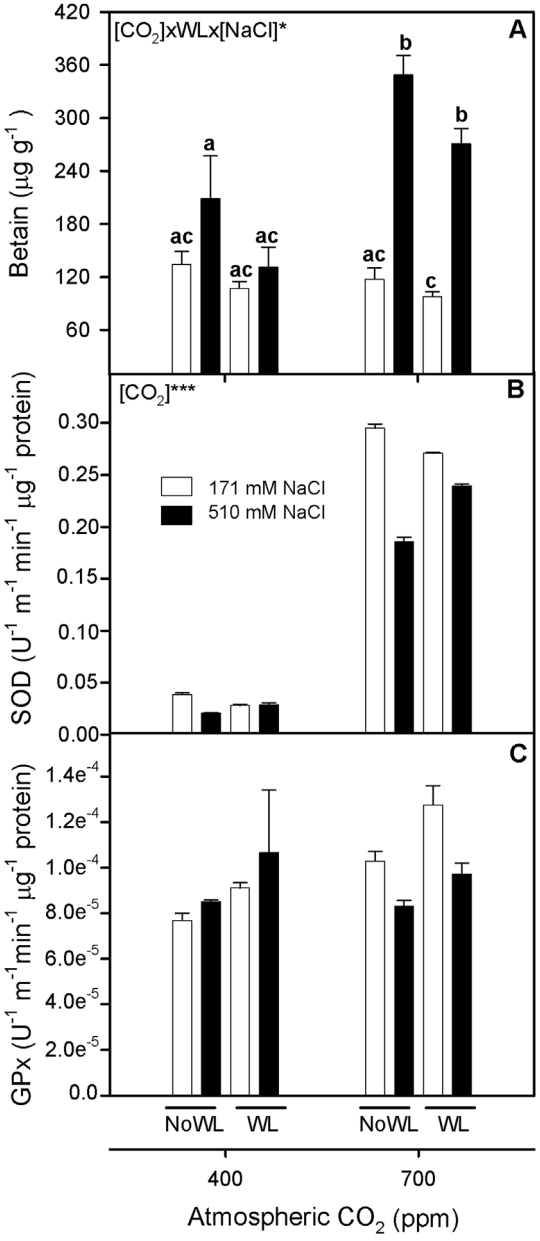

Fig. 6. Betain (A), superoxide dismutase (SOD) (B) and guaiacol peroxidase (GPx) (C) enzymatic activities in randomly selected, primary branches of *Salicornia ramosissima* in response to treatment with two of NaCl concentrations (171 and 510 mM) and with water logging (WL) and with no water logging (no WL) at 400 and 700 ppm CO_2 after 45d of treatment. Values represent mean ± SE, n = 3. Different letters indicate means that are significantly different from each other (GLM, [CO_2] x WLx [NaCl]; LSD test, $P < 0.05$). [CO_2],WL, [NaCl] or [CO_2] x WL x [NaCl] in the corner of the panels indicate main or interaction significant effects ($^{*}P < 0.01$, $^{**}P < 0.001$, $^{***}P < 0.0001$).

(2007) previously highlighted, the increment in CO_2 atmospheric concentration allow plants to acquire the carbon needed with less stoma aperture rising the efficiency in the use of water for them. A very similar trends have been previously reported in *S. ramosissima* and in other halophytes (Geissler et al., 2009a, 2009b; 2015; Mateos-Naranjo et al., 2010a, 2010b; Pérez-Romero et al., 2018) in response to NaCl excess and in combination with soil flooding conditions (Lenssen et al., 1995). Nevertheless, to our knowledge, this is the first study where CO_2 enrichment beneficial effects under coexisted root flooding conditions could be also ascribed to up-regulation of some component involved in PSII energy transport chain, accumulation of osmoprotective compounds and the modulation of fatty acids profiles, as indicated our multivariate statistical approach.

Despite the existence of widely documented deleterious effect of prolonged water logging (Mateos-Naranjo et al., 2007; Cao et al., 2017; Ullah et al., 2017) and NaCl concentration excess (Flexas et al., 2004; Mateos-Naranjo and Redondo-Gómez, 2016) on photochemical apparatus our results showed a different scenario. It could be seen that in general PS II and its antennae complex were not affected by any of the tested stressful treatments. As it was indicated by the similarities in F_v/F_m, Φ_{PSII}, Area, δR0, φ_{P0}, Ψ_0, φ_{E0}, ABS/CS, TR/CS and ET/CS values between all experimental treatments. Nevertheless, plants exposed to 700 ppm CO_2 + WL + 510 mM NaCl presented the higher P_G, N and Sm values, which indicate that their reaction centres had lower re-oxidation rates and thus were able to generate electrons from photons in higher amounts per unit of time (Duarte et al., 2017). Moreover, the lack of difference in electron transport flux (ET/CS) suggests that the electron transport chain can deal with this increased number of electrons, derived from higher P_G, N and Sm values, and therefore under normal conditions it would be working at sub-saturated conditions. Hence, the positive impact of atmospheric CO_2 enrichment on photochemical apparatus of *S. ramosissima* could be ascribed to the enhanced of the efficiency for energy transport, avoiding the accumulation of energy excess, which could contribute to reduce the risk of oxidative stress due to the accumulation of reactive oxygen species (ROS). In fact, the lower risk of ROS production was supported by the decrease in ETR_{max}/A_N ratio recorded in *S. ramosissima* plants grown at 700 ppm CO_2 + WL + 510 mM NaCl compared with their non-CO_2 supplied counterparts. This ratio could be considered as an indicator of the potential ROS stress that plants are subjected to and derived from a possible lack of carbon units correspondent to the number of electrons generated (Salazar-Parra et al., 2012; Hussin et al., 2017). Together with the maintenance of energy transport efficiency, the accumulation of different protection compounds as osmocompatible solutes or the modulation of the anti-oxidative stress enzymes machinery was also in the basis of the redox-balance maintenance. Therefore, compounds such as betain are known to be produced by plants to cope with salinity or drought stress (Moradi et al., 2017). In this study, betain concentration showed a clear pattern of increment in relation with the atmospheric CO_2 in plants grown under stressful conditions. In addition, there was modulation effect, driven from an atmospheric CO_2 enrichment, in certain anti-oxidant enzymes of *S. ramosissima* as SOD. This enzyme showed higher activity levels compared their 400-ppm CO_2 counterpart contributing to cope with oxidative stress in greater extent.

Finally, the ameliorative effect of atmospheric CO_2 fertilization on *S. ramosissima* physiological responses under coexistence of water logging and salt excess was also supported by fatty acids profiles. Fatty acids profile has been suggested as useful biomarker for abiotic stress in halophytes species, such as *Spartina maritima*, *Spartina patens, Halimione portulacoides* and *Sarcocornia fruticosa*, and its levels are highly related to the photosynthetic functioning of these species (Duarte et al., 2017, 2018a; 2018b). Our results revealed that generally at elevated CO_2 concentrations there was a decrease in unsaturated/saturated ratio for all WL and salinity treatments, due to a major decrease in C18:3. A direct action of ROS production during stress exposition with the augmentation of the membrane lipid peroxidation has been described, which could led to a decrease in the C18:2 and C18:3 relative contents (Ouariti et al., 1997; Upchurch, 2008). In addition, it is well known that in photosynthetic tissues the C18:3 fatty acid is mostly associated with the galactolipids monogalactosyldiacylglycerol (MGDG) and digalactosyldiacylglycerol (DGDG), which are fundamental for the correct function of photosynthesis (Mizusawa and Wada, 2012). Hence, tissues with low amount of these kind of lipids (and consequently low C18:3 content) have disrupted photosynthetic membranes and a complete impairment of photochemical processes (Kobayashi et al., 2007;

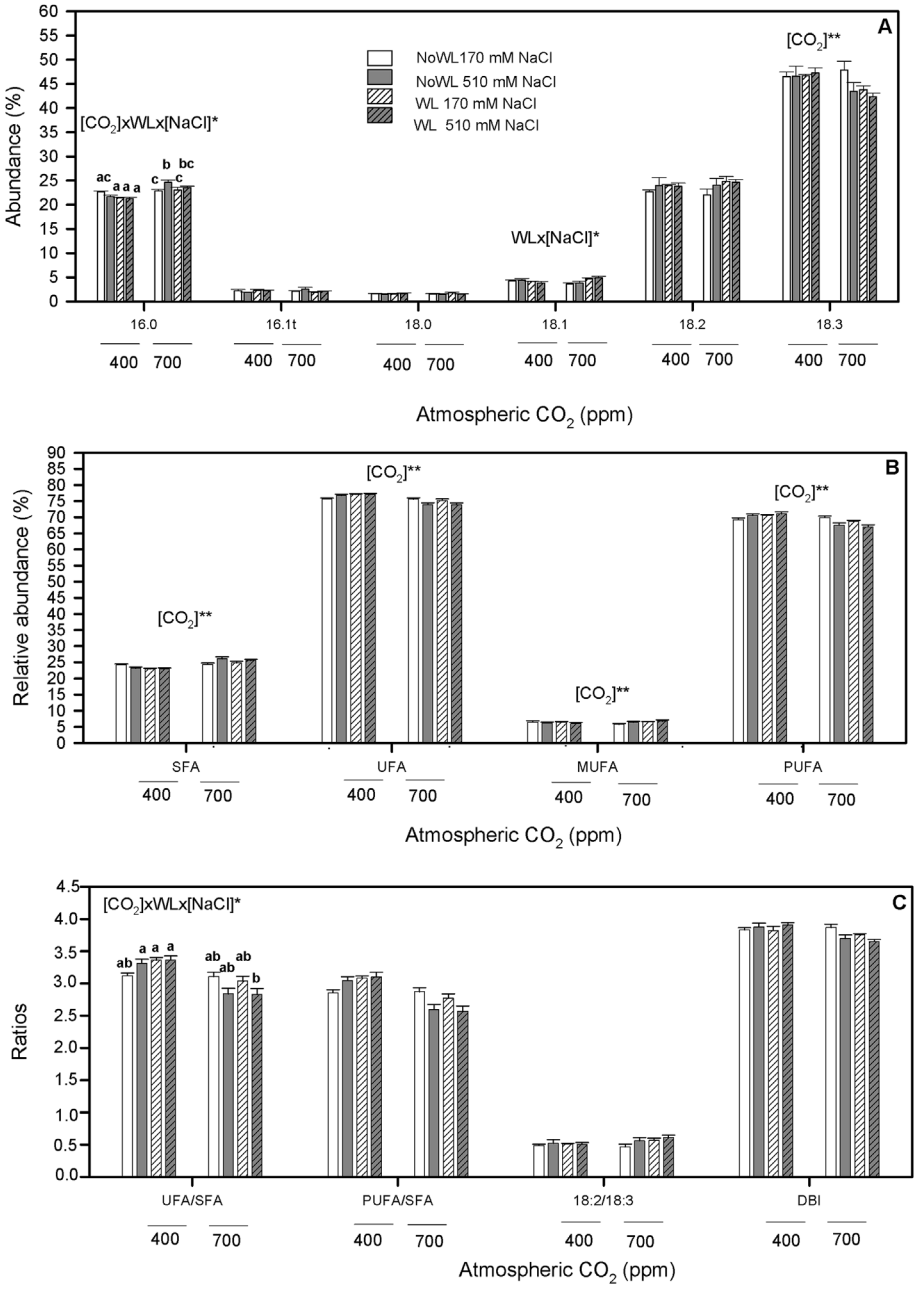

Fig. 7. Palmitic acid (16:0), palmitoleic acid (16:1t), stearic acid (18:0), oleic acid (18:1), linoleic acid (18:2) and omega-3 (18:3) abundance (A); saturated (SFA), unsaturated (UFA), monounsaturated (MUFA) and polyunsaturated (PUFA) relative abundance (B); unsaturated-saturated fatty acids (UFA/SFA), polyunsaturated-saturated fatty acids (PUFA/SFA), linoleic acid-omega-3 fatty acids (18:2/18:3) ratios and double-bond index (DBI) (C) calculated in randomly selected primary branches of *Salicornia ramosissima* in response to treatment with two of NaCl concentrations (171 and 510 mM) and with water logging (WL) and with no water logging (noWL) at 400 and 700 ppm CO_2 after 45d of treatment. Values represent mean ± SE, n = 5. Different letters indicate means that are significantly different from each other (GLM, [CO_2] x WLx [NaCl]; LSD test, $P < 0.05$). [CO_2],WL, [NaCl] or [CO_2] x WL x [NaCl] in the corner of the panels indicate main or interaction significant effects ($^{*}P < 0.01$, $^{**}P < 0.001$, $^{***}P < 0.0001$).

Aronsson et al., 2008). However, according to Duarte et al. (2017) in the halophyte *Aster tripolium* we found that there was not a correlation between the decrease in C18:3 and photosynthetic apparatus performance. The lack of relationship was ascribe to an adaptation in which the polyunsaturated fatty acids (more specific the C18:3) decrease to cope with salinity stress (Duarte et al., 2017). In addition, we found that plants grown at 700 ppm CO_2 showed higher values for the fatty acid C16:0. This increment would be associated to an improvement in the PS II function since this fatty acid presents an important role in this component of the photosynthetic pathway (Gounaris and Barber, 1985; Duarte et al., 2017).

5. Conclusion

This experiment confirmed previous work that had demonstrated atmospheric CO_2 enrichment ameliorative effect on salinity tolerance of *S. ramosissima* (Pérez-Romero et al., 2018). Nevertheless, we found that this positive effect under synergistic root-flooding was mainly owing to upregulation its energy sink capacity, as indicated the increment in the rate of reaction centre turnover, relative pool size of PQ and the connectivity beween PSII units, together with the already previously described increment in carbon assimilation and water balance capacity. In addition, our results indicated that the beneficial effect of CO_2 concentration was ascribed to a better modulation of the antioxidant enzyme machinery and of the betain accumulation on tissues to cope with oxidative stress, as well as to a great presence in saturated fatty acids, which would be associated with the aforementioned improvement in the PSII function.

CRediT authorship contribution statement

Jesús Alberto Pérez-Romero: Conceptualization, Investigation, Methodology, Formal analysis, Writing – original draft. **Bernardo Duarte:** Formal analysis, Supervision, Writing – review & editing. **Jose-Maria Barcia-Piedras:** Data curation, Methodology. **Ana Rita Matos:** Formal analysis, Resources. **Susana Redondo-Gómez:** Conceptualization, Project administration. **Isabel Caçador:** Formal analysis, Resources. **Enrique Mateos-Naranjo:** Formal analysis, Conceptualization, Supervision, Writing – review & editing.

Acknowledgements

This work has been funded by Ministerio de Economía y Competitividad (MINECO Project CGL2016-75550-R cofunded by FEDER). J.A Pérez-Romero thanks Ministerio de Educación, Cultura y Deporte for its personal financial support (FPU014/03987). We are grateful University of Seville Greenhouse General Services (CITIUS) for its collaboration. The authors would also like to thank to the "Fundação para a Ciência e a Tecnologia" for funding the research in the Marine and Environmental Sciences Centre (MARE) and the Intercollegiate Studies Institute throughout the projects UID/MAR/04292/2013 and UID/MULTI/04046/2013 respectively. B. Duarte investigation was supported by FCT throughout a Posdoctoral grant (SFRH/BPD/115162/2016). We are grateful to Pablo Robles Delgado for revision of the English text of this manuscript.

References

Aronsson, H., Schottler, M.A., Kelly, A.A., Sundqvist, C., Dormann, P., Karim, S., Jarvis, P., 2008. Monogalactosyldiacylglycerol deficiency in *Arabidopsis* affects pigment composition in the prolamellar body and impairs thylakoid membrane energization and photoprotection in leaves. Plant Physiol. 148 (1), 580–592.

Bergmeyer, H.U., 1974. Methods of enzymatic analysis, vol. 4 Academic Press. http://www.sciencedirect.com/science/book/9780120913046.

Bernacchi, C.J., Leakey, A.D., Heady, L.E., Morgan, P.B., Dohleman, F.G., McGrath, J.M., et al., 2006. Hourly and seasonal variation in photosynthesis and stomatal conductance of soybean grown at future CO2 and ozone concentrations for 3 years under fully open-air field conditions. Plant Cell Environ. 29 (11), 2077–2090.

Bradford, M.M., 1976. A rapid and sensitive method for the quantification of micro-gram quantities of protein utilizing the principle of protein–dye binding. Anal. Biochem. 72, 248–254.

Calvo, O.C., Franzaring, J., Schmid, I., Müller, M., Brohon, N., Fangmeier, A., 2017. Atmospheric CO2 enrichment and drought stress modify root exudation of barley. Global Change Biol. 23 (3), 1292–1304.

Cao, Y., Ma, C., Chen, G., Zhang, J., Xing, B., 2017. Physiological and biochemical responses of *Salix integra* Thunb. under copper stress as affected by soil flooding. Environ. Pollut. 225, 644–653.

Davy, A.J., Bishop, G.F., Costa, C.S.B., 2001. *Salicornia* L. (*Salicornia pusilla* J. Woods, *S. ramosissima* J. Woods, *S. europaea* l., *S. obscura* P. W. Ball & Tutin, *S. nitens* P. W. Ball & Tutin, *S. fragilis* P. W. Ball & Tutin, P. W. Ball & Tutin and *S. dolichostachya* Moss). J. Ecol. 89, 681–707.

Duarte, B., Santos, D., Marques, J.C., Caçador, I., 2013. Ecophysiological adaptations of two halophytes to salt stress: photosynthesis, PS II photochemistry and anti-oxidant feedback - Implications for resilience in climate change. Plant Physiol. Biochem. 67, 178–188.

Duarte, B., Santos, D., Silva, H., Marques, J.C., Caçador, I., Sleimi, N., 2014. Light–dark O_2 dynamics in submerged leaves of C_3 and C_4 halophytes under increased dissolved CO_2: clues for saltmarsh response to climate change. AoB Plants 6 plu067. http://doi.org/10.1093/aobpla/plu067.

Duarte, B., Goessling, J.W., Marques, J.C., Caçador, I., 2015. Ecophysiological constraints of *Aster tripolium* under extreme thermal events impacts: Merging biophysical, biochemical and genetic insights. Plant Physiol. Biochem. 97, 217–228.

Duarte, B., Cabrita, M.T., Gameiro, C., Matos, A.R., Godinho, R., Marques, J.C., Caçador, I., 2017. Disentangling the photochemical salinity tolerance in *Aster tripolium* L.: connecting biophysical traits with changes in fatty acid composition. Plant Biol. 19 (2), 239–248.

Duarte, B., Carreiras, J., Pérez-Romero, J.A., Mateos-Naranjo, E., Redondo-Gómez, S., Matos, A.R., Redondo-Gómez, S., Marques, J.C., Caçador, I., 2018a. Halophyte fatty acids as biomarkers of anthropogenic-driven contamination in Mediterranean marshes: Sentinel species survey and development of an integrated biomarker response (IBR) index. Ecol. Indicat. 87, 86–96.

Duarte, B., Matos, A.R., Marques, J.C., Caçador, I., 2018b. Leaf fatty acid remodeling in the salt-excreting halophytic grass *Spartina patens* along a salinity gradient. Plant Physiol. Biochem. 124, 112–116.

Flexas, J., Bota, J., Loreto, F., Cornic, G., Sharkey, T.D., 2004. Diffusive and metabolic limitations to photosynthesis under drought and salinity in C3 plants. Plant Biol. 6 (3), 269–279.

Ghannoum, O., Von Caemmerer, S., Ziska, L.H., Conroy, J.P., 2000. The growth response of C4 plants to rising atmospheric CO2 partial pressure: A reassessment. Plant Cell Environ. 23 (9), 931–942.

Geissler, N., Hussin, S., Koyro, H.W., 2009a. Elevated atmospheric CO2 concentration ameliorates effects of NaCl salinity on photosynthesis and leaf structure of *Aster tripolium* L. J. Exp. Bot. 60 (1), 137–151.

Geissler, N., Hussin, S., Koyro, H.W., 2009b. Interactive effects of NaCl salinity and elevated atmospheric CO2 concentration on growth, photosynthesis, water relations and chemical composition of the potential cash crop halophyte *Aster tripolium* L. Environ. Exp. Bot. 65 (2–3), 220–231.

Geissler, N., Hussin, S., El-Far, M.M.M., Koyro, H.W., 2015. Elevated atmospheric CO2 concentration leads to different salt resistance mechanisms in a C3 (*Chenopodium quinoa*) and a C4 (*Atriplex nummularia*) halophyte. Environ. Exp. Bot. 118, 67–77.

Gounaris, K., Barber, J., 1985. Isolation and characterisation of a photosystem II reaction centre lipoprotein complex. FEBS Lett. 188, 68–72.

Grieve, C.M., Grattan, S.R., 1983. Rapid assay for determination of water soluble quaternary ammonium compounds. Plant Soil 70, 303.

Hoagland, D.R., Arnon, D.I., 1938. The water culture method for growing plants without soil. Calif. Agric. Ext. Serv. Circ. 347, 32.

Hussin, S., Geissler, N., El-Far, M.M.M., Koyro, H.W., 2017. Effects of Salinity and Short-Term Elevated Atmospheric CO 2 on the Chemical Equilibrium between CO 2 Fixation and Photosynthetic Electron Transport of *Stevia rebaudiana* Bertoni. Plant Physiol. Biochem. 118, 178–186. http://linkinghub.elsevier.com/retrieve/pii/S0981942817302085.

IPCC, 2001. In: Watson, R.T., the Core Writing Team (Eds.), Climate Change 2001: Synthesis Report. A Contribution of Working Groups I, II, and III to the Third Assessment Report of the Integovernmental Panel on Climate Change. Cambridge University Press, Cambridge, United Kingdom, and New York, NY, USA 398 pp.

IPCC, 2007. In: Core Writing Team, Pachauri, R.K., Reisinger, A. (Eds.), Climate Change 2007: Synthesis Report. Contribution of Working Groups I, II and III to the Fourth Assessment Report of the Intergovernmental Panel on Climate Change. IPCC, Geneva, Switzerland 104 pp.

Kobayashi, K., Kondo, M., Fukuda, H., Nishimura, M., Ohta, H., 2007. Galactolipid synthesis in chloroplast inner envelope is essential for proper thylakoid biogenesis, photosynthesis, and embryogenesis. Proc. Natl. Acad. Sci. U. S. A 104 (43), 17216–17221.

Lenssen, G., Lamers, J., Stroetenga, M., Rozema, J., 1993. Interactive effects of atmospheric CO2 enrichment, salinity and flooding on growth of C 3 (*Elymus athericus*) and C 4 (*Spartina anglica*) salt marsh species. Vegetatio 104/105 (0), 379–388.

Lenssen, G.M., van Duin, W.E., Jak, P., Rozema, J., 1995. The response of *Aster tripolium* and *Puccinellia maritima* to atmospheric carbon dioxide enrichment and their interactions with flooding and salinity. Aquat. Bot. 50 (2), 181–192. http://doi.org/10.1016/0304-3770(95)00453-7.

Marklund, S., Marklund, G., 1974. Involvement of the superoxide anion radical in the autoxidation of pyrogallol and a conveniente assay for superoxide dismutase. Eur. J. Biochem. 47, 469–474.

Marshall, H.L., Geider, R.J., Flynn, K.J., 2000. A mechanistic model of photoinhibition. New Phytol. 145 (2), 347–359.

Mateos-Naranjo, E., Redondo-Gómez, S., Silva, J., Santos, R., Figueroa, M.E., 2007. Effect of Prolonged Flooding on the Invader *Spartina densiflora* Brong. J. Aquat. Plant Manag. 45 (2), 121–123.

Mateos-Naranjo, E., Redondo-Gomez, S., Alvarez, R., Cambrolle, J., Gandullo, J., Figueroa, M.E., 2010a. Synergic effect of salinity and CO2 enrichment on growth and photosynthetic responses of the invasive cordgrass Spartina densiflora. J. Exp. Bot. 61 (6), 1643–1654.

Mateos-Naranjo, E., Redondo-Gómez, S., Andrades-Moreno, L., Davy, A.J., 2010b. Growth and photosynthetic responses of the cordgrass *Spartina maritima* to CO_2 enrichment and salinity. Chemosphere 81, 725–731.

Mateos-Naranjo, E., Redondo-Gómez, S., 2016. Inter-population differences in salinity tolerance of the invasive cordgrass *Spartina densiflora*: Implications for invasion process. Estuar. Coast 39, 98–107.

Matos, A.R., Hourton-Cabassa, C., Ciçek, D., Rezé, N., Arrabaça, J.D., Zachowski, A., Moreau, F., 2007. Alternative oxidase involvement in cold stress response of *Arabidopsis thaliana fad2* and *FAD3+* cell suspensions altered in membrane lipid composition. Plant Cell Physiol. 48 (6), 856–865.

Mizusawa, N., Wada, H., 2012. The role of lipids in photosystem II. Biochim. Biophys. Acta Bioenerg. 1817 (1), 194–208.

Moradi, P., Ford-Lloyd, B., Pritchard, J., 2017. Metabolomic approach reveals the biochemical mechanisms underlying drought stress tolerance in thyme. Anal. Biochem. 527, 49–62.

Ouariti, O., Boussama, N., Zarrouk, M., Cherif, A., Ghorbal, M.H., 1997. Cadmium- and copper-induced changes in tomato membrane lipids. Phytochemistry 45 (7), 1343–1350.

Pérez-Romero, J.A., Redondo-Gomez, S., Mateos-Naranjo, E., 2016. Growth and photosynthetic limitation analysis of the Cd-accumulator *Salicornia ramosissima* under excessive cadmium concentrations and optimum salinity conditions. Plant Physiol. Biochem. 109, 103–113.

Pérez-Romero, J.A., Idaszkin, Y., Barcia-Piedras, J.M., Duarte, B., Redondo-Gomez, S., Caçador, I., Mateos-Naranjo, E., 2018. Disentangling the effect of atmospheric CO2 enrichment on the halophyte Salicornia ramosissima J. Woods physiological performance under optimal and suboptimal saline conditions. Plant Physiol. Biochem. 127, 617–629.

Redondo-Gómez, S., Mateos-Naranjo, E., Figueroa, M.E., Davy, A.J., 2010. Salt stimulation of growth and photosynthesis in an extreme halophyte, *Arthrocnemum macrostachyum*. Plant Biol. 12 (1), 79–87.

Reed, D.J., 2002. Sea-level rise and coastal marsh sustainability: geological and ecological factors in the Mississippi delta plain. Geomorphology 48 (1–3), 233–243.
Robredo, A., Pérez-López, U., de la Maza, H.S., González-Moro, B., Lacuesta, M., Mena-Petite, A., Muñoz-Rueda, A., 2007. Elevated CO2 alleviates the impact of drought on barley improving water status by lowering stomatal conductance and delaying its effects on photosynthesis. Environ. Exp. Bot. 59 (3), 252–263.
Rozema, J., 1993. Plant-responses to atmospheric carbon-dioxide enrichment - interactions with some soil and atmospheric conditions. Vegetatio 104, 173–190.
Salazar-Parra, C., Aquirreolea, J., Sánchez-Díaz, M., Irigoyen, J.J., Morales, F., 2012. Climate Change (elevated CO2, elevated temperature and moderate drought) triggers the antioxidant enzymes' response of grapevine cv. tempranillo, avoiding oxidative damage. Physiol. Plantarum 144 (2), 99–110.
Slama, I., M'Rabet, R., Ksouri, R., Talbi, O., Debez, A., Abdelly, C., 2015. Water deficit stress applied only or combined with salinity affects physiological parameters and antioxidant capacity in *Sesuvium portulacastrum*. Flora −Morphol. Distrib. Funct. Ecol. Plants 213, 69–76.
Schreiber, U., Schliwa, U., Bilger, W., 1986. Continuous recording of photochemical and non-photochemical chlorophyll fluorescence quenching with a new type of modulation fluorometer. Photosynth. Res. 10 (1–2), 51–62.
Strasser, R.J., Tsimilli-Michael, M., Srivastava, A., 2004. Analysis of the chlorophyll a fluorescence transient. In: Papageorgiou, G.C., Govindjee (Eds.), Chlorophyll a Fluorescence: A Signature of Photosynthesis. Springer Netherlands, Dordrecht, pp. 321–362.
Ullah, I., Waqas, M., Khan, M.A., Lee, I.J., Kim, W.C., 2017. Exogenous ascorbic acid mitigates flood stress damages of *Vigna angularis*. Applied Biological Chemistry 60 (6), 603–614.
Upchurch, R.G., 2008. Fatty acid unsaturation, mobilization, and regulation in the response of plants to stress. Biotechnol. Lett. 30 (6), 967–977.
Yang, Z., Xie, T., Liu, Q., 2014. Physiological responses of *Phragmites australis* to the combined effects of water and salinity stress. Ecohydrology 7, 420–426.